eFood
Vol. 1(4); August (2020), pp. 326–331
DOI: https://doi.org/10.2991/efood.k.200727.001; eISSN 2666-3066
https://www.atlantis-press.com/journals/efood

Research Article

Characterizations of a Food Decapeptide Chelating with Zn(II)

Weiwei Fan[1,2], Zhenyu Wang[1], Zhishen Mu[3], Ming Du[1], Lianzhou Jiang[4], Hesham R. EI-Seedi[5,6], Cong Wang[1,3,*]

[1]*Center of Experimental Instrument, School of Food Science and Technology, Dalian Polytechnic University, Dalian 116034, China*
[2]*School of Bioengineering, Dalian University of Technology, Dalian 116024, China*
[3]*Inner Mongolia Mengniu Dairy Industry (Group) Co., Ltd., Hohhot 010000, China*
[4]*College of Food Science, Northeast Agricultural University, Harbin 150030, China*
[5]*Pharmacognosy Group, Department of Medicinal Chemistry, Uppsala University, Biomedical Centre, Uppsala 75 123, Sweden*
[6]*International Research Center for Food Nutrition and Safety, Jiangsu University, Zhenjiang, 212013, China*

ARTICLE INFO

Article History
Received 14 May 2020
Accepted 20 July 2020

Keywords
Peptide
zinc
binding sites
molecular docking
structure

ABSTRACT

Walnut proteins and peptides have been reported to have great zinc-carrying activity. In this study, the decapeptide EPNGLLLPQY (WP-10) derived from walnut protein has been prepared to figure out zinc binding mechanisms and structure–activity relationships. The space-conformation of this peptide has converted after being chelated with Zn(II). As to secondary structure, the β-sheet structure of the peptide turned into α-helix and β-turn structure. According to the atomic absorption spectra analysis, one peptide could bind with one Zn(II) via four different binding sites. The signals of different groups in infrared spectroscopy have shifted before and after chelation, and the major functional groups of this peptide involved in chelation are $-NH_2$ and –C=O. GLU1, PRO2, ASP3, GLU4, and LEU6, and the molecular docking proved their participation in the chelating with Zn(II).

1. INTRODUCTION

Zinc is an important mineral that is involved in physiological metabolism, and functions in more than 300 metalloenzymes as a catalytic component ensuring the structural integrity of proteins [1]. Moreover, zinc has a vital influence on the immune system, as it is required for the activation of different kinds of immune cells [2]. Besides, zinc plays an important role in maintaining cell reproduction, gene expression, regulatory function, neurogenesis and neurotransmission [3,4]. But zinc cannot be synthesized in the body, and human zinc reserves are limited. Therefore, biological zinc must be continuously supplied from the individuals diet [5]. Zinc deficiency can seriously affect the immune system and destroy the redox balance of the body, leading to immune dysfunction, neurological decline, and the occurrence of some pathological diseases [6].

At present, zinc can be obtained from mineral salts and metal chelating agents [7]. However, mineral salts have poor bioavailability due to the inhibition of dietary components such as tannins, phytates, and dietary fibers [8,9]. Therefore, it is necessary to develop alternatives that can improve the bioavailability of zinc. Subsequently, more attention has been paid to the study of new supplements of zinc, such as zinc-binding proteins or peptides as functional food.

Pioneering studies have shown that expressed proteins bear metal-coordinating side chains or incorporate such groups [10], and the same applies to food-derived peptides. A great number of food-derived peptides with metal chelating abilities have been identified such as the sesame protein [11], whey protein [12], milk protein [13], Antarctic krill protein [14], amyloid protein [15] and walnut protein [16]. Furthermore, food-derived peptides can be easily digested and absorbed due to having a small molecular weight and a simple structure. However, the activity of the walnut-derived polypeptide with zinc chelation has been hardly reported.

The study presented here demonstrates the structure–activity relationship of Zn(II) and walnut-derived polypeptides share after chelation. In our team's previous research, several peptides were isolated and identified from walnut protein. Among them, Glu-Pro-Asn-Gly-Leu-Leu-Leu-Pro-Gln-Tyr (WP-10) showed metal ion chelating activity. The aim of this study was to prepare zinc-chelating peptides (purified synthetic walnut-derived polypeptides) and provide the theoretical basis behind using zinc-chelating peptides from walnut protein as a functional food ingredient.

2. MATERIALS AND METHODS

2.1. Materials and Chemicals

The walnut peptide WP-10 was synthesized from Cellman Biotech Limited Corporation (Hefei, China). Zinc chloride buffer solutions of varying pH levels and all other reagents were purchased from Damao Chemical Reagent Co. Ltd. (Tianjin, China).

*Corresponding author. Email: *yuanque@163.com*
Peer review under responsibility of the *International Association of Dietetic Nutrition and Safety*

2.2. Preparation of the Zinc-Chelating Peptide

WP-10 (0.2 mmol/mL) was dissolved in a Tris-HCl buffer (0.05 mol/L, pH 5.0) containing $ZnCl_2$. The centrifuge tube containing the mixture was placed in a constant temperature shaking water bath at 47°C for 80 min. After that, the free zinc ion was removed by dialysis for 24 h using a 100 Da molecular weight dialysis bag made of semi-permeable membrane, and collected retentates (containing chelated zinc). Additionally, a part of it was lyophilized as a complete chelate for the following study.

2.3. Zinc Chelating Capacity Analysis

The free zinc content in the supernatant was evaluated by flame atomic absorption spectrometry (ZA3000, HITACHI, Japan) according to Wu, Wenfei and Smichowski's methods with some modifications [17,18], the chelated zinc content was calculated. The experiments were performed in triplicates and data was presented as the mean of each repeated experiment.

2.4. Ultraviolet–Visible Spectroscopy

In order to testify the occurrence of the zinc-chelating peptide reaction and investigate the functional mechanism between the peptide and peptide-zinc chelates, the absorbance values were recorded in the wavelength range from 200 to 1100 nm with an Ultraviolet–Visible (UV–Vis) spectrophotometer (F-2700, HITACHI, Japan). The zinc-chelating peptide and pure peptide were dissolved in a 0.1 mol/L Tris-HCl buffer (pH 7.4). Besides, samples were put in a quartz cuvette with a path length of 0.5 cm [19–21].

2.5. Circular Dichroism Spectroscopy

The secondary structure of the zinc-chelating peptide and pure peptide was investigated with a circular dichroism (CD) spectrophotometer (J-1500, Jasco, Japan) and the zinc-chelating peptide was compared to the pure peptide. The spectra of the zinc-chelating peptide and pure peptide were recorded in the wavelength range from 190 to 260 nm with a scanning rate of 20 nm/min, and a 1 nm bandwidth. In these experiments, the data was represented as the average of three independent scans with the control CD signal subtracted [22].

2.6. Fourier Transform Infrared Spectroscopy

The zinc-chelating peptide and pure peptide were inspected by Fourier Transform Infrared Spectroscopy (FTIR) (Frontier, Perkin Elmer, USA). One milligram of the sample was mixed with 100 mg of dried KBr, pulverized in an agate mortar, and then pressed into a transparent round shape [23]. The spectra were recorded in the wavenumber region of 4000–400 per cm with a resolution of 4 per cm and an average scan of 16 times [24]. The potential zinc-chelating sites were deduced from the significant shifts in absorption bands [16].

2.7. Molecular Dynamics Simulation

The discovery Studio 2017 R2 software with minor modifications was used to conduct molecular docking between WP-10 and zinc ions. The amino acid sequence of peptides was entered and the peptide structure was pretreated with the Prepare Protein tool. The structures of the ligands were generated by the DS 2017 R2 software and the Full Minimization tool was utilized to give the minimized energy. The peptide structure was processed with the clean and prepare protein program to model missing loop regions, remove water, add hydrogen, and optimize the bond length. The docking sites have a spherical center with a center diameter of 8 Å as the active site to cover the docking region. The docking program was carried out using the partial flexibility program CDOCKER protocol. Evaluation of molecular docking results was based on CDOCKER energy scores, interaction sites, and interaction force types [25,26].

3. RESULTS AND DISCUSSION

3.1. Zinc Chelating Capacity of Peptide

Zinc chelating capacity of peptide was shown in Figure 1. The amount of chelated Zn(II) on the WP-10 increased when the concentration of Zn(II) increased. The zinc chelating capacity did not increase significantly when zinc concentration reached 1.5 μmol/L. The reason may be that it is already saturated. Therefore, zinc ion concentration was one of the most important factors affecting the chelating capacity.

3.2. Ultraviolet–Visible Spectroscopy Analysis

As the curve shown in Figure 2, there are peaks in 280 and 220 nm, respectively as determined by the intensity and dislocation change of UV–Vis spectroscopy. As we all know, Tyrosine (Tyr) can absorb

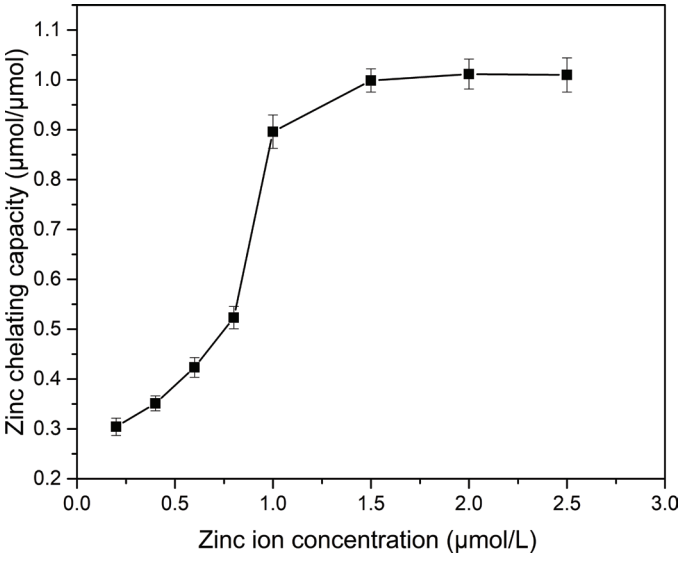

Figure 1 | Effects of zinc ion concentration on zinc chelating capacity. The zinc chelating capacity was determined by flame atomic absorption spectrometry. All the samples were determined three times and the data were reported as mean ± SD.

ultraviolet light at 278 nm, Tryptophan (Trp) can absorb ultraviolet light at 279 nm, Phenylalanine (Phe) can absorb ultraviolet light at 259 nm. The peak detected in 280 nm was small, which was attributed to lack of Phe, Tyr and Trp. After chelating interactions, the peak value slightly reduced, which was explained by the facts that some of Tyr in WP-10 were buried after chelation with Zn(II). These results were corresponded to the results of Figure 1. As for the peaks in 220 nm, it also decreased after chelating. It indicated that WP-10 were chelated to Zn(II) and the content of free peptides was decreased.

3.3. Circular Dichroism Spectroscopy Analysis

In circular dichroism spectrum analysis, if a negative peak ranged between 190 and 220 nm, it indicates that the peptide has a random structure. Similar results were found as for β-sheet structure, when negative peak ranges from 210 to 225 nm. As shown in Figure 3, the curve of circular dichroism spectrum for WP-10 had a negative peak at 190–225 nm. Therefore, it may have β-sheet and random structures. Moreover, it could be found that WP-10 contains mostly the structure of random and β-sheet which was 79.6% and 20.4% in the peptide, respectively.

When the WP-10 was chelated with Zn(II), its molecular structure changed accordingly. It could be found that a positive peak ranged from 190 to 195 nm while a negative peak from 195 to 220 nm, which indicated that α-helix and β-turn presented after WP-10 chelated with Zn(II), while β-sheet disappeared. The proportions of α-helix, β-turn and random structures were 18.5%, 17.8%, and 63.8%, respectively.

Compared to these two results, it was verified that the effect of Zn(II) on the structure of WP-10 was consistent with the results of UV–Vis spectroscopy analysis. In a Zn(II) rich system, Zn(II) chelating WP-10 was a process that destroyed the β-sheet structure and reconstituted it to α-helix and β-turn in WP-10 resolution. In this process, a part of random structures was involved in this conversion.

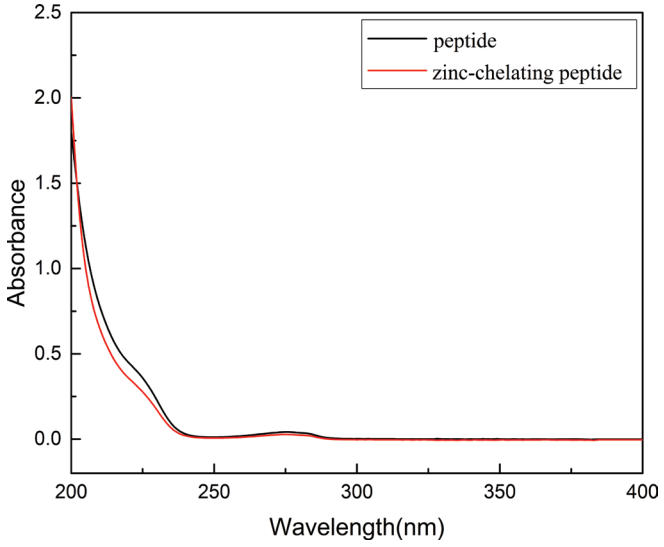

Figure 2 | UV–Vis spectrum of the decapeptide and zinc-chelating peptide. The WP-10 and zinc-chelating peptide were dissolved in Tris-HCl buffer (0.1 mol/L, pH 7.4). The spectra were recorded between 200 and 1100 nm with a scan speed of 20 nm/min.

3.4. Fourier Transform Infrared Spectroscopy Analysis

As shown in Figure 4, the wave number (WN) region of infrared spectrogram (IR) fingerprint spectrum was ranged from 650 to 1350 per cm. It could be found that the waveforms of WP-10 and zinc-chelating peptide complexes were significantly different while waveforms among the chelated peptides in different Zn(II) concentration were similar. These fingerprint spectrums could be used to distinguish this peptide whether chelated with Zn(II) or not. Combined with Figures 1 and 2, the IR and structure of the pure peptide, the peaks of functional groups, such as C–C(O), NH, RNH_2, –CH, $–CH_3$, C=O, could be identified. The amide-I vibration (C=O stretching vibration, 1690–1630 per cm) and amide-II vibration (N–H bending (40–60%) and C–N stretching vibrations (18–40%), 1655–1590 per cm) were the most dominant vibrational modes of amides [27]. The peak of C=O in 1650 per cm disappeared after chelation. It indicated that the oxygen atom of C=O may be chelated with Zn(II). The peaks of RNH_2 and NH in 3450 and 3300 per cm shifted to high WN respectively, blue-shift. According to the structure of WP-10, this may be because the nitrogen atom of RNH_2 and NH was chelated with Zn(II) leading to the increase of electronegativity around the nitrogen atom. The peaks of

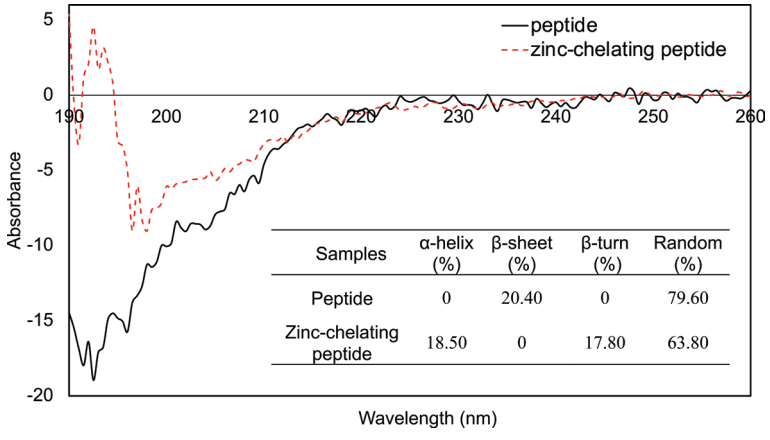

Samples	α-helix (%)	β-sheet (%)	β-turn (%)	Random (%)
Peptide	0	20.40	0	79.60
Zinc-chelating peptide	18.50	0	17.80	63.80

Figure 3 | CD spectrum of the decapeptide and zinc-chelating peptide. The WP-10 and zinc-chelating peptide were dissolved in Milli-Q water to a final concentration of 0.20 mmol/mL. The spectra were recorded between 190 and 260 nm with a scan speed of 20 nm/min.

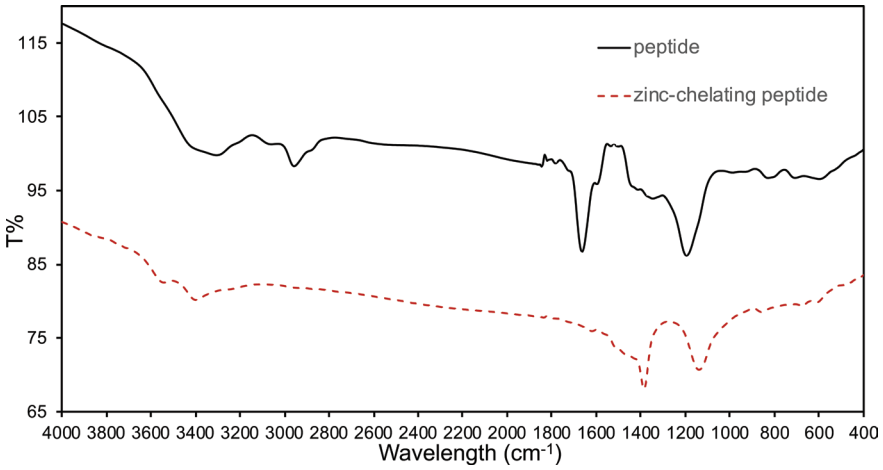

Figure 4 | Infrared spectrogram of the decapeptide and zinc-chelating peptide. The spectra were recorded between 4000 and 400 per cm at a resolution of 4 per cm with an average of 16 scans.

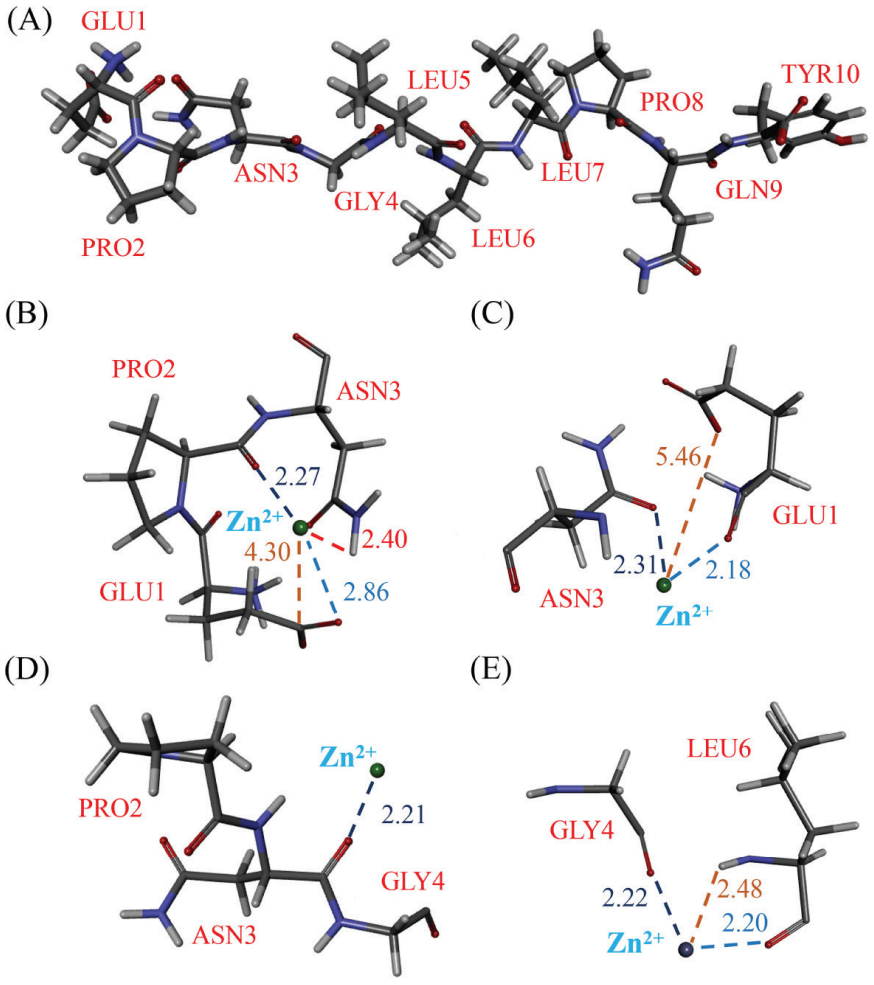

Figure 5 | Molecular docking simulation of peptide chelated with zinc. (A) was the structure of peptide after energy minimization. (B–E) were the chelation sites.

C–C(O) in 1200 per cm, represented aromatic acyl halide, shifted to low WN, known as red-shift. It is owing to the presence of the phenolic hydroxyl group of the tyrosine forming the hydrogen bond. This result confirmed that the absorption value of UV decreased at 220 nm and 280 nm after chelation. The FTIR spectra of peptide-zinc(II) complex in walnut showed similar changes [16].

3.5. Molecular Dynamic Simulation of Zinc-Chelating Peptide

Molecular docking predicts the interactions between ligands and receptors by calculating interaction such as interaction energies, binding sites, and other information. As shown in Figure 5, the

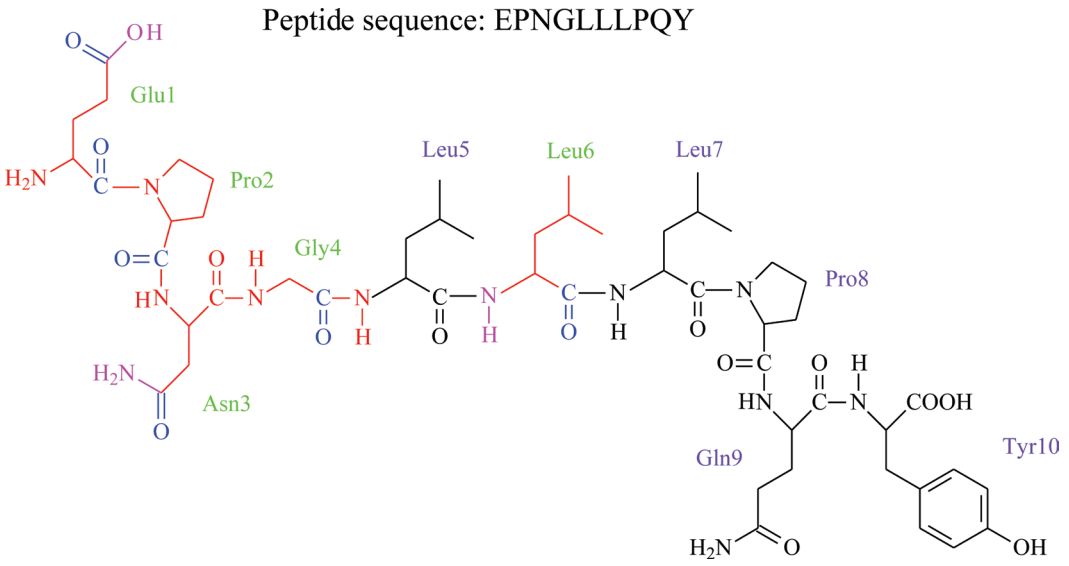

Figure 6 | The chemical structure diagram of peptide. The structures marked with red color were represented the amino acids that participated in the chelation (marked with green name). The structures marked with black color were represented the amino acids that do not participated in the chelation (marked with purple name). The groups marked with blue color were represented the functional groups that participated in the chelation. The groups that may affect the chelation results were marked with pink color (repulsive force).

structure of WP-10 after energy minimization was used to simulate the docking of Zn(II). The docking results indicated that there were four possible binding sites of Zn(II) in WP-10. GLU1, PRO2, and ASN3 ($G_{LU1}P_{RO2}A_{SN3}$) formed one of sites. GLU1 and ASN3 ($G_{LU1}A_{SN3}$) formed one site. ASN3 (A_{SN3}) formed another site, while GLY4 and LEU6 ($G_{LY4}L_{EU6}$) form the last one. However, the chelation strength is different at different sites. The conclusion was also demonstrated in Figure 1.

In Figure 6, the functional groups that play a major role in chelation was shown. As to WP-10, carbonyl group was the main functional groups interacting with Zn(II). The hydroxy group of GLU1 and the amidogen of ASN3 and LEU6 also could affect the chelation. According to these results, the structure of WP-10 could be changed and combined by site-specific mutagenesis for further application.

4. CONCLUSION

The WP-10 has an outstanding Zn(II) binding affinity. There are four sites in WP-10 that could bind with Zn(II) in Zn(II) rich environments. The maximal ratio of WP-10 chelated with Zn(II) was 1:1. GLU1, PRO2, ASN3, GLY4, and LEU6 were the main amino acids to form the chelation sites. The main groups involved in chelation were carbonyl groups. Some of the hydroxyl and amidogen groups also contribute to the chelation. The results from this study indicate that it is feasible to produce natural metal chelating using WP-10 peptides from walnut protein.

CONFLICTS OF INTEREST

The authors declare they have no conflicts of interest.

AUTHORS' CONTRIBUTION

WF contributed in writing original draft preparation. LJ and HRE contributed in writing review and editing. MD and CW contributed in supervision. ZW and ZM contributed in funding acquisition.

ACKNOWLEDGMENTS

This study was financially supported by the Basic Research Program of Liaoning Education Department (2017J080) and the National Natural Science Foundation of China (31371805).

REFERENCES

[1] McCall KA, Huang C, Fierke CA. Function and mechanism of zinc metalloenzymes. J Nutr 2000;130:1437S–46S.
[2] Prasad AS. Discovery of human zinc deficiency: 50 years later. J Trace Elem Med Biol 2012;26:66–9.
[3] Maret W, Sandstead HH. Zinc requirements and the risks and benefits of zinc supplementation. J Trace Elem Med Biol 2006;20:3–18.
[4] Hambidge M. Human zinc deficiency. J Nutr 2000;130;1344S–9S.
[5] El-Din AMG, Hassan ASH, El-Behairy SA, Mohamed EA. Impact of zinc and iron salts fortification of buffalo's milk on the dairy product. World J Dairy Food Sci 2012;7:21–7.
[6] Aquilanti L, Kahraman O, Zannini, E, Osimani, A, Silvestri, G, Ciarrocchi, F, et al. Response of lactic acid bacteria to milk fortification with dietary zinc salts. Int Dairy J 2012;25:52–9.
[7] Hurrell R. How to ensure adequate iron absorption from iron-fortified food. Nutr Rev 2002;60:S7–S15.

[8] Lee SH, Song KB. Purification of an iron-binding nona-peptide from hydrolysates of porcine blood plasma protein. Process Biochem 2009;44:378–81.
[9] Lönnerdal B. Dietary factors influencing zinc absorption. J Nutr 2000;130:1378S–83S.
[10] Tavenor NA, Murnin MJ, Horne WS. Supramolecular metal-coordination polymers, nets, and frameworks from synthetic coiled-coil peptides. J Am Chem Soc 2017;139:2212–15.
[11] Wang C, Li B, Ao J. Separation and identification of zinc-chelating peptides from sesame protein hydrolysate using IMAC-Zn^{2+} and LC-MS/MS. Food Chem 2012;134:1231–8.
[12] Udechukwu MC, Downey B, Udenigwe CC. Influence of structural and surface properties of whey-derived peptides on zinc-chelating capacity, and *in vitro* gastric stability and bioaccessibility of the zinc-peptide complexes. Food Chem 2018;240:1227–32.
[13] Rana B, Kaushik R, Kaushal K, Arora S, Kaushal A, Gupta S, et al. Physicochemical and electrochemical properties of zinc fortified milk. Food Biosci 2018;21:117–24.
[14] Hou H, Wang S, Zhu X, Li Q, Fan Y, Cheng D, et al. A novel calcium-binding peptide from Antarctic krill protein hydrolysates and identification of binding sites of calcium-peptide complex. Food Chem 2018;243:389–95.
[15] Faller P, Hureau C, La Penna G. Metal ions and intrinsically disordered proteins and peptides: from Cu/Zn amyloid-β to general principles. Acc Chem Res 2014;47:2252–9.
[16] Liao W, Lai T, Chen L, Fu J, Sreenivasan ST, Yu Z, et al. Synthesis and characterization of a walnut peptides-zinc complex and its antiproliferative activity against human breast carcinoma cells through the induction of apoptosis. J Agric Food Chem 2016;64:1509–19.
[17] Wu W, Li B, Hou H, Zhang H, Zhao X. Isolation and identification of calcium-chelating peptides from Pacific cod skin gelatin and their binding properties with calcium. Food Funct 2017;8:4441–8.
[18] Smichowski P, Londonio A. The role of analytical techniques in the determination of metals and metalloids in dietary supplements: a review. Microchem J 2018;136:113–20.
[19] Wang X, Gao A, Chen Y, Zhang X, Li S, Chen Y. Preparation of cucumber seed peptide-calcium chelate by liquid state fermentation and its characterization. Food Chem 2017;229:487–94.
[20] Huang SL, Zhao LN, Cai X, Wang SY, Huang YF, Hong J, et al. Purification and characterisation of a glutamic acid-containing peptide with calcium-binding capacity from whey protein hydrolysate. J Dairy Res 2015;82:29–35.
[21] Chen D, Liu ZY, Huang WQ, Zhao YH, Dong SY, Zeng MY. Purification and characterisation of a zinc-binding peptide from oyster protein hydrolysate. J Funct Foods 2013;5:689–97.
[22] Nakatsuka N, Barnaby SN, Tsiola A, Fath KR, Williams BA, Banerjee IA. Self-assembling peptide assemblies bound to ZnS nanoparticles and their interactions with mammalian cells. Colloid Surf B Biointerfaces 2013;103:405–15.
[23] Zhang Z, Zhou F, Liu X, Zhao M. Particulate nanocomposite from oyster (*Crassostrea rivularis*) hydrolysates via zinc chelation improves zinc solubility and peptide activity. Food Chem 2018;258:269–77.
[24] Hajji L, Boukir A, Assouik J, Kerbal A, Kajjout M, Doumenq P, et al. A multi-analytical approach for the evaluation of the efficiency of the conservation–restoration treatment of Moroccan historical manuscripts dating to the 16th, 17th, and 18th centuries. Appl Spectrosc 2015;69:920–38.
[25] Vats C, Dhanjal JK, Goyal S, Bharadvaja N, Grover A. Computational design of novel flavonoid analogues as potential AChE inhibitors: analysis using group-based QSAR, molecular docking and molecular dynamics simulations. Struct Chem 2015;26:467–76.
[26] Fu Y, Alashi AM, Young JF, Therkildsen M, Aluko RE. Enzyme inhibition kinetics and molecular interactions of patatin peptides with angiotensin I-converting enzyme and renin. Int J Biol Macromol 2017;101:207–13.
[27] Zhou J, Wang X, Ai T, Cheng X, Guo HY, Teng GX, et al. Preparation and characterization of β-lactoglobulin hydrolysate-iron complexes. J Dairy Sci 2012;95:4230–6.